

Channel capacity comparison of different system concepts for mmWave

Kilian Roth ^{*†}, Javier Garcia[†], Jawad Munir[†], Michael Faerber^{*}, Josef A. Nossek[†]

^{*} Next Generation and Standards, Intel Deutschland GmbH, Neubiberg, Germany

Email: {kilian.roth, michael.faerber}@intel.com

[†] Institute for Circuit Theory and Signal Processing, Technical University Munich, Munich, Germany

Email: {kilian.roth, javier.garcia, jawad.munir, josef.a.nossek}@tum.de

Abstract—For 5G it will be important to leverage the available millimeter wave spectrum. Communication at high carrier frequencies requires antenna arrays at both the base and mobile station. A 1-bit analog to digital converter can effectively reduce the complexity and power consumption of the analog receiver frontend. This is especially interesting in the context of large antenna arrays with a sizable signal bandwidth. The RF receiver frontend power consumption of analog beamforming, full resolution ADC digital beamforming, and 1-bit quantized digital beamforming are compared. This power model consists of components designed for the 60 GHz band. With this power model systems with equal power consumption, and therefore different numbers of antennas, are compared in terms of channel capacity. In the low SNR regime the performance of the system with 1-bit quantization outperforms the ones with full resolution ADC digital beamforming and analog beamforming.

I. INTRODUCTION

For the next generation mobile broadband standard higher carrier frequencies are being considered [1]. These frequencies are in the range of 6 to 100 GHz. In general this frequency range is referred to as millimeter wave (mmW), even though it contains the lower centimeter wave range. The major advantage is the large available bandwidth. To fully leverage the spectrum while being power-efficient, the base band (BB) and radio frontend (RFE) capabilities must be drastically changed.

The use of high carrier frequencies above 6 GHz will go hand in hand with the implementation of massive antenna arrays [1], [2]. The support of a large number of antennas and RFE at the mobile and base station requires radical, new frontend designs. To attain a similar link budget, the effective antenna aperture of a mmWave system must be comparable to current systems operating at carrier frequencies below 6 GHz. Therefore, an antenna array at the base and mobile station might be necessary. Since the antenna gain and therefore the directivity increases with the aperture, an antenna array is the only solution to achieve a high effective aperture while maintaining an omnidirectional coverage.

Current LTE systems have limited amount of antennas at the base and mobile stations. Since the bandwidth is narrow, the power consumption of having a receiver RF chain with high resolution A/D converter at each antenna is still feasible. For future mmWave mobile broadband systems a much larger bandwidth [3] and a large number of antennas are being considered [1]. The survey [4] shows that A/D converters with

a large sampling frequency, and medium number of effective bits consume a considerable amount of power. The ADC can be considered as the bottleneck of the receiver [5].

The antenna array combined with the large bandwidth is a huge challenge for the hardware implementation, the power consumption will limit the design space. At the moment analog or hybrid beamforming are considered as a possible solution to reduce the power consumption. Analog or hybrid beamforming systems highly depend on the calibration of the analog components. Another major disadvantage is the dependency on the alignment of the Tx and Rx beams of the base and mobile stations. If a high antenna gain is needed the beamwidth is very small. This makes the acquisition and constant alignment of the optimal beams in a changing environment very challenging [6], [7] and [8].

For a mmWave system at the receiver of the mobile or base station, digital beamforming has a prohibiting high power consumption. Therefore a solution that offers the full flexibility of MIMO with constrained power consumption is to use a simple radio frontend, with low resolution A/D conversion, at each antenna [9], [10] and [11]. In the extreme case that would mean utilizing a 1-bit ADC for the inphase and quadrature component of the signal. This receiver architecture has the advantage that an AGC is not needed, thus the VGA can be replaced by a much simpler limiting amplifier. Because the 1-bit quantization represents a major non-linearity at the end of the receiver chain, the requirements on the linearity and dynamic range of the whole receiver chain is reduced. This has the potential to save additional power, without any further compromises in terms of performance and flexibility.

The contribution of this paper is to show the relative performance of the different receiver architectures taking the power consumption into account. The power consumption is based on designs reported for the 60 GHz band. Only low cost, low power CMOS implementations are considered. The relative performance between the different receiver architectures is expected remain the same for a wider frequency range. The implementation complexity of the digital signal processing is also expected to be similar, and is therefore not taken into account.

Our paper is organized as follows: First the signal model is described. Then the power model of the different receiver architectures are presented. Afterwards the channel capacity

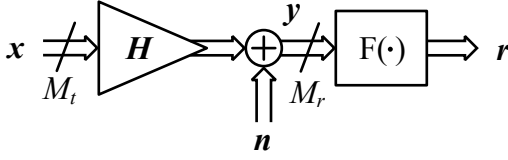


Fig. 1. Signal Model.

of the different systems are derived. In the end the channel capacity of the systems with equal power consumption are compared.

Throughout the paper we use boldface lower and upper case letters to represent column vectors and matrices. The term $a_{m,l}$ is the element on row m and column l of matrix \mathbf{A} and a_m is the m th element of vector \mathbf{a} . The expressions \mathbf{A}^* , \mathbf{A}^T , \mathbf{A}^H , and \mathbf{A}^{-1} represent the complex conjugate, the transpose, the Hermitian, and the inverse of the operand.

II. SIGNAL MODEL

The signal model is shown in Figure 1. The symbols \mathbf{x} , \mathbf{H} , \mathbf{n} , and \mathbf{y} represent the transmit signal, channel, noise, and receive signal of a system. M_t transmit and M_r receive antennas are used. The operation $F(\cdot)$ is different for the analog/hybrid beamforming and low/high resolution digital beamforming. In the case of analog/hybrid beamforming it is equal to multiplying with a matrix \mathbf{W} :

$$\mathbf{r}_{a/h} = F_{a/h}(\mathbf{y}) = \mathbf{W}\mathbf{y}. \quad (1)$$

The matrix \mathbf{W} is representing the phase shifts at each antenna element. Each entry of the matrix is a phase rotation with magnitude one. The matrix \mathbf{W} has M_{RFC} rows and M_r columns. Analog beamforming can be seen as the special case of hybrid beamforming with $M_{RFC} = 1$.

For digital beamforming with high resolution the distortion generated by the A/D conversion is negligible, thus r_∞ is equal to \mathbf{y} :

$$\mathbf{r}_\infty = F_\infty(\mathbf{y}) = \mathbf{y}. \quad (2)$$

In the case of 1-bit quantization $F(\cdot)$ is equal to the quantization operation $Q_1(\cdot)$:

$$\mathbf{r}_1 = F_1(\mathbf{y}) = Q_1(\mathbf{y}). \quad (3)$$

The 1-bit quantization operation $Q_1(\cdot)$ is defined as follows:

$$Q_1(\mathbf{y}) := \text{sign}(\Re(\mathbf{y})) + j \cdot \text{sign}(\Im(\mathbf{y})). \quad (4)$$

The $\text{sign}(\cdot)$ function is operating separately on each element of a vector or matrix. It is defined as:

$$\text{sign}(a) := \begin{cases} 1, & a > 0 \\ -1, & a \leq 0 \end{cases}. \quad (5)$$

III. POWER CONSUMPTION MODEL

In a future 5G millimeter Wave mobile broadband system it will be necessary to utilize large antenna arrays. Since the power consumptions scales linear with number of antennas, it could get enormous. It is therefore important to compare the power consumption of different receiver architectures. In this section we compare the power consumption of analog/hybrid beamforming to digital beamforming, and the proposed digital beamforming architecture with 1-bit quantization.

Since the spectrum in the 60 GHz band can be accessed without a license, it got significant attention. Especially the WiGig (802.11ad) standard operating in this band increased the transceiver RF hardware R&D activities. Many chips were reported from industry and academia. Thus it is safe to assume that the design reached a certain maturity, and performance figures derived from them represent the performance that is possible for a low cost CMOS implementation today.

According to the discussion in [12] baseband or IF phase shifting in contrast to RF phase shifting is assumed. This has the advantage of increased accuracy, decreased insertion loss, and reduced gain mismatch. In [12] the authors showed that the power consumption for a low number of antennas per RF-chain is equivalent to a system utilizing RF phase shifters.

All three systems utilize the same direct conversion receiver (Figure 2). For each system we assume that the Local Oscillator (LO) shared by the whole system. After the signals are converted into inphase and quadrature component of the analog baseband signal (BBI and BBQ), the additional circuit is different. The analog baseband circuit of the full resolution digital beamforming system only consists of a variable gain amplifier (VGA), and a full resolution ADC for the I and Q path at each antenna (Figure 3). In contrast the 1-bit quantized digital beamforming does not need a VGA, because we do not need to adjust the gain to utilize the full dynamic range of the ADC. The circuit consists of a limiting amplifier (LA) and the 1-bit ADC (Figure 5) for I and Q. Figure 4 shows the analog baseband block diagram of a radio frontend chain. Here the signals of N antennas are phase shifted and then combined by an analog combiner. N is defined as the number of receive antennas M_r divided by the number for RF chains M_{RFC} . Afterwards the I and Q path of the combined signal are amplified with a VGA and converted into the digital domain by a high resolution ADC. Depending on the total number of receive antennas M_r and RF-chains M_{RFC} this system is denoted as analog or hybrid beamforming. The number of antennas is always larger or equal to the number of RF-chains $M_r \geq M_{RFC}$. For $M_{RFC} = 1$ the system is using pure analog beamforming, otherwise a hybrid beamforming architecture is used.

The power consumption of each component, including a reference, are shown in Table I. A LO with a power consumption as low as 22.5mW is reported in [13]. The power consumption of a LNA, a mixer including a quadrature-hybrid coupler, and a VGA are reported in [14] as 5.4, 0.5, and 2mW. The 90° hybrid and the clock buffer reported in [15] have a combined power

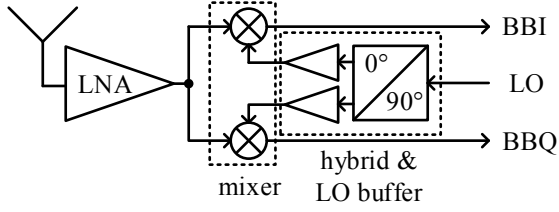


Fig. 2. Common circuit blocks of all systems.

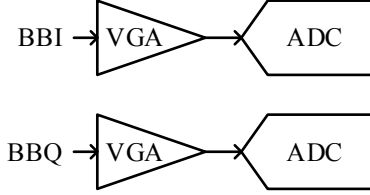


Fig. 3. Baseband digital beamforming system.

consumption of 3 mW. The power consumption of the mixer reported in [16] is as low as 0.3mW. The survey in [4] always gives a good overview of state of the art ADCs. It shows the parameters effective number of bits (ENOB), sampling rate, and power consumption. From the survey and examples like [17] and [18] we can extrapolate that for an ADC with about 8 ENOB and 2.5GS/s the power consumption is at best around 10mW. A limiting amplifier (LA) that consumes 0.8mW is reported in [19]. In the 1-bit quantized system the LA (aka. Schmitt trigger) is already producing a digital signal, therefore the 1-bit ADC can be replaced by a flip flop (FF). The power consumption of a FF is negligible compared to the rest of the circuit.

From the power consumption of the components it is possible to compute the power consumption of the 4 receiver types

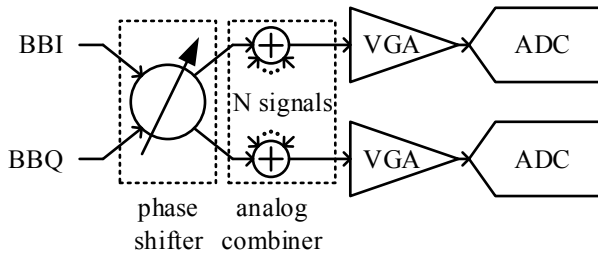


Fig. 4. Baseband analog/hybrid beamforming system.

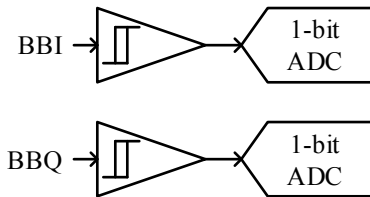


Fig. 5. Baseband 1-bit digital beamforming system.

TABLE I
COMPONENTS WITH POWER CONSUMPTION.

label	component	power consumption	reference
P_{LO}	LO	22.5mW	[13]
P_{LNA}	LNA	5.4mW	[14]
P_M	Mixer	0.3mW	[16]
P_H	90° hybrid and LO buffer	3mW	[15]
P_{LA}	LA	0.8mW	[19]
P_1	1-bit ADC	0mW	
P_{PS}	phase shifter (PS)	2mW	[20] [12]
P_{VGA}	VGA	2mW	[14]
P_{ADC}	ADC	10mW	[4], [17] and [18]

digital beamforming (P_{DBF}), analog beamforming (P_{ABF}), hybrid beamforming (P_{HBF}), and 1-bit quantized digital beamforming ($P_{1-bitBF}$). The formulas for calculating the power consumption are:

$$P_{DBF} = P_{LO} + M(P_{LNA} + P_H + 2P_M + 2P_{VGA} + 2P_{ADC}), \quad (6)$$

$$P_{HBF} = P_{LO} + M(P_{LNA} + P_H + 2P_M + P_{PS}) + M_{RFC}(2P_{VGA} + 2P_{ADC}), \quad (7)$$

$$P_{1-bitBF} = P_{LO} + M(P_{LNA} + P_H + 2P_M + 2P_{LA} + 2P_1). \quad (8)$$

Analog beamforming can be seen as the special case of hybrid beamforming with only one RF-chain ($M_{RFC} = 1$).

A receiver directly designed for the 1-bit quantization digital beamforming systems is very likely to improve the power consumptions even further. Due to the 1-bit quantization at the end of the receiver, the linearity required of the circuits before is greatly reduced. This would enable specialized designs to improve the performance in terms of power consumption.

In this analysis we showed that, with state of the art components, the per antenna power consumption for the architecture with high resolution ADC is around 3 times higher than for the system utilizing 1-bit ADCs. For the rest of the evaluation we use this power model to compare the different systems with equal power consumption.

IV. ACHIEVABLE RATE WITH DIFFERENT RECEIVER ARCHITECTURES

In this section the channel capacity expressions that are used to compare the systems are shown. All expressions assume perfect channel knowledge at the transmitter and receiver (full CSIT and CSIR). In the case of 1-bit quantized MIMO the expression is a lower bound of the channel capacity. For the rest of the paper the the average SNR γ at the receive antenna

is used. The average receive SNR γ is defined as the average receive power divided by the noise power.

$$\gamma = \frac{P_t}{\sigma_n^2}. \quad (9)$$

With P_t being the transmit power. This formula hold true under the assumption that the average signal gain of the channel is equal to one. We also assume that the noise is complex circular symmetric Gaussian distributed with zero mean, variance σ_n^2 , and independent at each antenna.

A. High resolution A/D MIMO

In the case without quantization the maximum rate is achieved by the waterfilling solution shown in [21]. The channel capacity is defined as:

$$R_{HDBF}(\mathbf{H}) = \sum_{i=1}^{\text{rank}(\mathbf{H})} \log_2 \left(1 + P_i \frac{D_i^2}{\sigma_n^2} \right). \quad (10)$$

D_i is the i th non zero singular value of the matrix \mathbf{H} . The power allocation P_i of the i th channel is derived from:

$$P_i = \max \left(\left(\mu - \frac{\sigma_n^2}{D_i^2} \right), 0 \right) \text{ and } \sum_{i=1}^{M_t} P_i = P_t. \quad (11)$$

The abbreviation HDBF stands for high resolution ADC digital beamforming.

B. Analog beamforming

For analog beamforming the input receive signal after the analog combining of the signals from all antennas can be described as:

$$y = \mathbf{w}_r^H (\mathbf{H} \mathbf{w}_t x + \mathbf{n}). \quad (12)$$

Here the symbols \mathbf{w}_t and \mathbf{w}_r represent the precoding and reception vector. In this paper the transmitter has no constraints and therefore \mathbf{w}_t can take any value. The use of analog beamforming is envisioned in many future mobile broadband systems, especially in the mmW frequency range ([22] and [23]). An analog beamforming receiver scans different spatial direction (beams) and then selects the configuration maximizing it's SNR. There are many different possibilities for selecting the optimal beam, e.g. 802.11ad is using a procedure based on exhaustive search [24].

For the evaluation we assume that the receiver utilizes an Uniform Linear Antenna Array (ULA) (Figure 6). If the distance between adjacent antenna elements is equal to half of the wavelength $d = \lambda/2$, the signal at adjacent antennas are phase shifted by ϕ .

$$\phi = \pi \sin(\theta). \quad (13)$$

This formula assumes that a planar wavefront is impinging at the antenna array, and that the modulated signal is narrow-band compared to the carrier frequency. With the constraint of observing only a single spatial direction, the receive vector \mathbf{w}_r for an ULA antenna array has to take the form:

$$\mathbf{w}_r^H = [1, e^{j\phi}, e^{j2\phi}, \dots, e^{j(M_r-1)\phi}]. \quad (14)$$

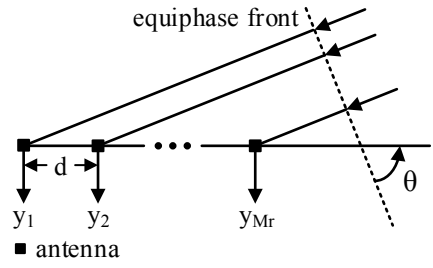


Fig. 6. Planar wavefront arriving at ULA antenna array.

The achievable rate of this system dependent on \mathbf{w}_r and \mathbf{w}_t is given by:

$$R_{ABF}(\mathbf{H}) = \log_2 \left(1 + \frac{|\mathbf{w}_r^H \mathbf{H} \mathbf{w}_t|^2}{M_r \sigma_n^2} \right). \quad (15)$$

Since \mathbf{w}_r has only entries with magnitude one and the noise is independent AWGN at each antenna, the total noise power $E[|\mathbf{w}_r^H \mathbf{n}|^2]$ is equal to $M_r \sigma_n^2$. Maximizing $R_{ABF}(\mathbf{H})$ is equivalent to maximizing $|\mathbf{w}_r^H \mathbf{H} \mathbf{w}_t|^2$. Given the optimal receive beamforming vector $\hat{\mathbf{w}}_r$ the optimization problem:

$$\max_{\mathbf{w}_t} |\hat{\mathbf{w}}_r^H \mathbf{H} \mathbf{w}_t|^2. \quad (16)$$

is solved by Maximum Ratio Transmission (MRT). The MRT vector $\hat{\mathbf{w}}_t$ dependent on reception vector \mathbf{w}_r in the following way:

$$\hat{\mathbf{w}}_t(\mathbf{w}_r) = \frac{\mathbf{H}^H \mathbf{w}_r}{\|\mathbf{H}^H \mathbf{w}_r\|_2}. \quad (17)$$

If we plug in 17 into 16 and consider that \mathbf{w}_r only depends on ϕ we get:

$$\max_{\phi} \frac{|\mathbf{w}_r^H(\phi) \mathbf{H} \mathbf{H}^H \mathbf{w}_r(\phi)|^2}{\|\mathbf{H}^H \mathbf{w}_r(\phi)\|_2^2} = \max_{\phi} \|\mathbf{w}_r^H(\phi) \mathbf{H}\|_2^2. \quad (18)$$

The spatial shift ϕ can only take values in the interval from $-\pi$ to π , therefore it is feasible to test the whole range of ϕ on a regular grid. The distance between two points in this grid must depend on the size of the receiver array. After the optimal point in the grid is found, a gradient based approach will lead to the optimal phase shift $\hat{\phi}$. The maximum rate is given by:

$$R_{ABF}(\mathbf{H}) = \log_2 \left(1 + \frac{\|\mathbf{w}_r^H(\hat{\phi}) \mathbf{H}\|_2^2}{M_r \sigma_n^2} \right). \quad (19)$$

C. 1-bit quantized MIMO

The channel capacity and different bound of the achievable rate of a MIMO system with 1-bit quantization at the receiver are shown in [8]. The lower bound derived in [25] is shown to be tight in the low SNR regime. Since we are mainly interested

TABLE II
POWER CONSUMPTION OF THE CHOSEN CONFIGURATION.

system	antennas	power consumption
HDBF	3	121.5mW
ABF	7	123.5mW
LDBF	10	128.5mW

in the low SNR, it is sufficient to use this lower bound of the achievable rate:

$$R_{LDBF}(\mathbf{H}) = \log_2 \left| \mathbf{I}_{M_t} + \frac{\gamma}{M_t} \mathbf{H}^H \text{diag} \left(\frac{1-\rho}{1+\rho \frac{\gamma}{M_t} \|\mathbf{h}_i\|_2^2} \right) \mathbf{H} \right|. \quad (20)$$

The vector \mathbf{h}_i is the i th row of the channel matrix \mathbf{H} . ρ represents the distortion factor that is dependent on the resolution, for 1-bit quantization $\rho = 0.3634$. The values for ρ are the minimum distortion introduced by a linear quantizer if the signal is Gaussian. A table for different resolutions can be found in [26]. LDBF stands for low resolution ADC digital beamforming.

D. Channel models

For the evaluation we use two simplified channel models. The first one is the classical i.i.d. Gaussian channel model. Here the each entry $h_{i,j}$ of the matrix \mathbf{H} is circular symmetric Gaussian distributed with zero mean and unit variance and all entries are generated independent of each other.

The second one is modeling different rays impinging on the receiver antenna array. To simplify the evaluation we assume that they arrive at the same time. Under the assumption of an ULA at the transmitter and receiver a channel consisting of L different rays can be modeled as:

$$\mathbf{H} = \frac{1}{\sqrt{L}} \sum_{l=1}^L \alpha(l) \mathbf{a}_r(\phi_r(l)) \mathbf{a}_t^T(\phi_t(l)). \quad (21)$$

The vectors $\mathbf{a}_r(\phi_r(l))$ and $\mathbf{a}_t(\phi_t(l))$ are the arrays steering vectors at the receiver and transmitter. The phase shift between the signal of adjacent antenna elements $\phi_r(l)$ and $\phi_t(l)$ of path l depend on the angle of arrival $\theta_r(l)$ and departure $\theta_t(l)$ as shown in Figure 6 and Equation 13.

$$\mathbf{a}_r^T(\phi_r(l)) = \left[1, e^{j\phi_r(l)}, e^{j2\phi_r(l)}, \dots, e^{j(M_r-1)\phi_r(l)} \right]. \quad (22)$$

The complex gains $\alpha(l)$ are circular symmetric Gaussian distributed with zero mean and unit variance. The angle of arrival $\theta_r(l)$ and departure $\theta_t(l)$ are uniform distributed in the range of $-\pi$ to π .

The main motivation of this channel model is to mimic the behavior of an actual mmWave channel. Compared to frequencies used for mobile broadband today, the channel in mmWave experiences a reduced spatial spread [7].

V. SIMULATION RESULTS

In this simulation based evaluation the 3 different systems are compared. These systems are:

- Analog beamforming (ABF)
- Digital beamforming with high resolution ADC (HDBF)
- Digital beamforming with 1-bit resolution ADC (LDBF)

Representatives of each systems type with equal power consumption of the receiver frontend, according to Section III, are generated. These representatives are compared in terms of the achievable rate and bounds on the achievable rate shown in Section IV. As shown in Table II at approximately the same power consumption we can utilize 3 receive antennas for HDBF, 7 antennas for ABF, and 10 antennas for LDBF. 1000 different channel realizations are generated. The achievable rates $R_{HDBF}(\mathbf{H})$, $R_{LDBF}(\mathbf{H})$, and $R_{ABF}(\mathbf{H})$ are calculated and averaged over the realizations.

Figure 7 shows that the low resolution ADC digital beamforming outperforms the other two systems in the low SNR regime. Here the channel matrix \mathbf{H} has Gaussian i.i.d. entries. It is important to stress that the rate for LDBF is in fact a lower bound to achievable rate. Especially in the medium to high SNR the bound was shown to be loose [8]. Gaussian i.i.d. channel coefficients represent a rich scattering environment, which might not be a valid assumption for a mmWave system. In Figure 8 the same antenna configurations are simulated with the simplified ray based channel model. We can see that even with a channel consisting of only 3 rays the result is the system shows a similar performance, but the advantage of the 1-bit quantized system is less dominant. In the case there are two transmitter antennas available the performance of the ABF system is better than the one of LDBF. Overall the simulation results verify the assumption that dependent on the channel the LDBF system could outperform the other systems in the low SNR regime at the same power consumption.

VI. CONCLUSION

The evaluation of the power consumption of the receiver RF frontend showed, that compared to analog beamforming or digital beamforming with high resolution ADC, the 1-bit quantized digital beamforming consumes less power for each utilized antenna. This evaluation is based on low cost low power components developed for 802.11ad (aka. WigiG) devices. For some system configuration and channels the 1-bit quantized system outperforms the other systems in the low SNR regime. Compared to a analog/hybrid beamforming system the main advantage of the low resolution ADC system lies in the fact that a beam alignment and tracking is not necessary. Additional optimization of the receiver hardware is possible for the 1-bit quantized system and could improve the power consumption even further.

ACKNOWLEDGMENT

This work was supported by the European Commission in the framework of the H2020-ICT-2014-2 project Flex5Gware(Grant agreement no. 671563).

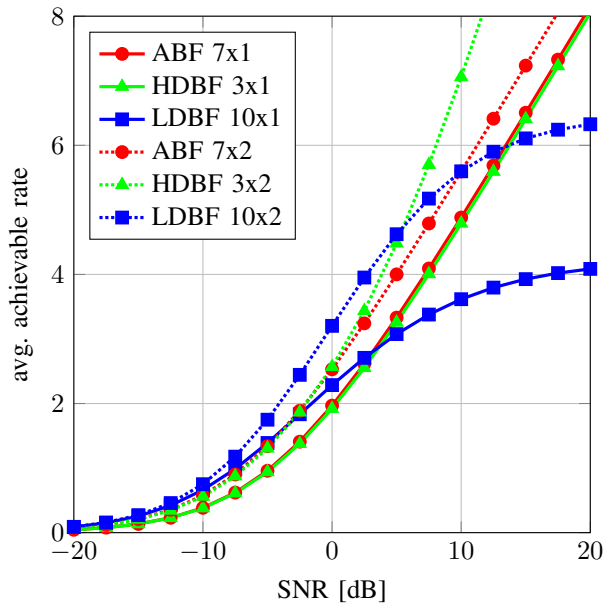


Fig. 7. Simulation with Gaussian i.i.d. channel coefficients.

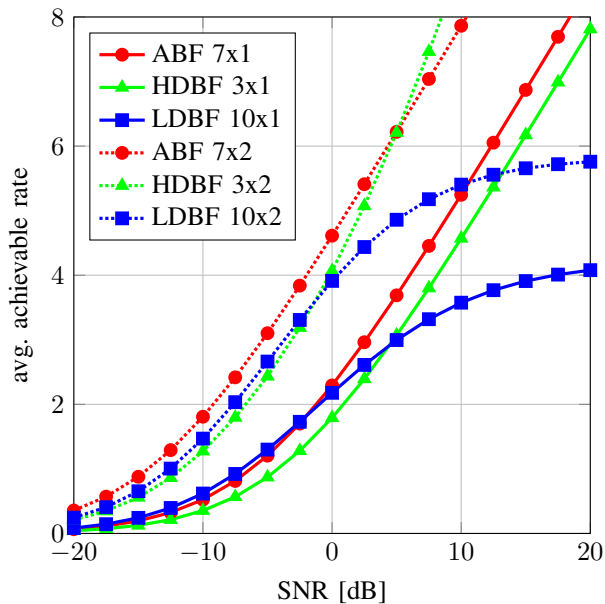


Fig. 8. Simulation with simplified ray based channel model with 3 path.

REFERENCES

- [1] F. Boccardi, R. Heath, A. Lozano, T. Marzetta, and P. Popovski, "Five Disruptive Technology Directions for 5G," *IEEE Communications Magazine*, vol. 52, no. 2, pp. 74–80, February 2014.
- [2] J. Andrews, S. Buzzi, W. Choi, S. Hanly, A. Lozano, A. Soong, and J. Zhang, "What Will 5G Be?" *IEEE Journal on Selected Areas in Communications*, vol. 32, no. 6, pp. 1065–1082, June 2014.
- [3] NGMN 5G Initiative Team, "5G White Paper," NGMN, TS, 2015. [Online]. Available: https://www.ngmn.org/uploads/media/NGMN_5G_White_Paper_V1_0.pdf
- [4] B. Murmann, "ADC Performance Survey 1997-2015," Tech. Rep., 2015. [Online]. Available: <http://www.stanford.edu/~murmman/adcsurvey.html>
- [5] J. Singh, O. Dabeer, and U. Madhoo, "Communication Limits with Low Precision Analog-to-Digital Conversion at the Receiver," *IEEE Transactions on Communications*, vol. 57, no. 12, pp. 3629–3639, December 2009.
- [6] C. Barati Nt., S. Hosseini, S. Rangan, P. Liu, T. Korakis, S. Panwar, and T. Rappaport, "Directional Cell Discovery in Millimeter Wave Cellular Networks," *IEEE Transactions on Wireless Communications*, vol. PP, no. 99, 2015.
- [7] T. Rappaport, R. Heath, R. Daniels, and J. Murdock, *Millimeter Wave Wireless Communications*, ser. Prentice Hall Communications Engineering and Emerging Technologies Series from Ted Rappaport. Pearson Education, 2014.
- [8] J. Mo and R. Heath, "Capacity Analysis of One-Bit Quantized MIMO Systems With Transmitter Channel State Information," *IEEE Transactions on Signal Processing*, vol. 63, no. 20, pp. 5498–5512, Oct 2015.
- [9] J. A. Nossek and M. T. Ivrlac, "Capacity and coding for quantized MIMO systems," in *IWCMC*, 2006.
- [10] A. Alkhateeb, J. Mo, N. Gonzalez-Prelcic, and R. Heath, "MIMO Precoding and Combining Solutions for Millimeter-Wave Systems," *IEEE Communications Magazine*, vol. 52, no. 12, pp. 122–131, December 2014.
- [11] A. Mezghani and J. Nossek, "On Ultra-Wideband MIMO Systems with 1-bit Quantized Outputs: Performance Analysis and Input Optimization," in *International Symposium on Information Theory, 2007. ISIT 2007. IEEE*, June 2007, pp. 1286–1289.
- [12] J. Chen, "Advanced Architectures for Efficient mm-Wave CMOS Wireless Transmitters," Ph.D. dissertation, EECS Department, University of California, Berkeley, May 2014. [Online]. Available: <http://www.eecs.berkeley.edu/Pubs/TechRpts/2014/EECS-2014-42.html>
- [13] K. Scheir, S. Bronckers, J. Borremans, P. Wambacq, and Y. Rolain, "A 52 GHz Phased-Array Receiver Front-End in 90 nm Digital CMOS," *IEEE Journal of Solid-State Circuits*, vol. 43, no. 12, pp. 2651–2659, Dec 2008.
- [14] Y. Shang, D. Cai, W. Fei, H. Yu, and J. Ren, "An 8mW ultra low power 60GHz direct-conversion receiver with 55dB gain and 4.9dB noise figure in 65nm CMOS," in *International Symposium on Radio-Frequency Integration Technology (RFIT), 2012 IEEE*, Nov 2012, pp. 47–49.
- [15] C. Marcu, "LO Generation and Distribution for 60GHz Phased Array Transceivers," Ph.D. dissertation, EECS Department, University of California, Berkeley, Dec 2011. [Online]. Available: <http://www.eecs.berkeley.edu/Pubs/TechRpts/2011/EECS-2011-132.html>
- [16] Y. Jin, J. Long, and M. Spirito, "A 7dB NF 60GHz-band millimeter-wave transconductance mixer," in *Radio Frequency Integrated Circuits Symposium (RFIC), 2011 IEEE*, June 2011, pp. 1–4.
- [17] H.-K. Hong, H.-W. Kang, D.-S. Jo, D.-S. Lee, Y.-S. You, Y.-H. Lee, H.-J. Park, and S.-T. Ryu, "26.7 A 2.6b/cycle-architecture-based 10b 1 JGS/s 15.4mWx time-interleaved SAR ADC with a multistep hardware-retirement technique," in *IEEE International Solid-State Circuits Conference - (ISSCC), 2015*, Feb 2015, pp. 1–3.
- [18] B.-R.-S. Sung, D.-S. Jo, I.-H. Jang, D.-S. Lee, Y.-S. You, Y.-H. Lee, H.-J. Park, and S.-T. Ryu, "26.4 A 21fJ/conv-step 9 ENOB 1.6GS/S 2x time-interleaved FATI SAR ADC with background offset and timing-skew calibration in 45nm CMOS," in *IEEE International Solid-State Circuits Conference - (ISSCC), 2015*, Feb 2015, pp. 1–3.
- [19] A. Oncu, B. Badalawa, and M. Fujishima, "60GHz-Pulse Detector Based on CMOS Nonlinear Amplifier," in *IEEE Topical Meeting on Silicon Monolithic Integrated Circuits in RF Systems, 2009. SiRF '09.*, Jan 2009, pp. 1–4.
- [20] L. Kong, "Energy-Efficient 60GHz Phased-Array Design for Multi-Gb/s Communication Systems," Ph.D. dissertation, EECS Department, University of California, Berkeley, Dec 2014. [Online]. Available: <http://www.eecs.berkeley.edu/Pubs/TechRpts/2014/EECS-2014-191.html>
- [21] E. T. Ar and I. E. Telatar, "Capacity of Multi-antenna Gaussian Channels," *European Transactions on Telecommunications*, vol. 10, pp. 585–595, 1999.
- [22] S. Sun, T. Rappaport, R. Heath, A. Nix, and S. Rangan, "MIMO for Millimeter-Wave Wireless Communications: Beamforming, Spatial Multiplexing, or Both?" *IEEE Communications Magazine*, vol. 52, no. 12, pp. 110–121, December 2014.
- [23] V. Venkateswaran and A.-J. van der Veen, "Analog Beamforming in MIMO Communications With Phase Shift Networks and Online Channel Estimation," *IEEE Transactions on Signal Processing*, vol. 58, no. 8, pp. 4131–4143, Aug 2010.

- [24] "IEEE Standard for Information technology–Telecommunications and information exchange between systems–Local and metropolitan area networks–Specific requirements–Part 11: Wireless LAN Medium Access Control (MAC) and Physical Layer (PHY) Specifications Amendment 3: Enhancements for Very High Throughput in the 60 GHz Band," *IEEE Std 802.11ad*, pp. 1–628, Dec 2012.
- [25] Q. Bai and J. A. Nossek, "Energy Efficiency Maximization for 5G Multi-Antenna Receivers," *Transactions on Emerging Telecommunications Technologies*, vol. 26, no. 1, pp. 3–14, 2015. [Online]. Available: <http://dx.doi.org/10.1002/ett.2892>
- [26] J. Max, "Quantizing for Minimum Distortion," *IRE Transactions on Information Theory*, vol. 6, no. 1, pp. 7–12, March 1960.